SPRITE detector characterization through impulse response testing

B.K. Anderson, G.D. Boreman*, K.J. Barnard* and A.E. Plogstedt

McDonnell Douglas Missile Systems Company
701 Columbia Blvd
Titusville, FL 32780

*University of Central Florida
CREOL/Electrical Engineering Department
Orlando, FL 32816

ABSTRACT

Various models of Signal Processing in the Element (SPRITE) detectors have been devised. Unfortunately, all of these models rely on parameters which vary significantly from detector to detector. These values are not supplied by detector manufacturers and are not readily available to system engineers. Therefore, a method of SPRITE detector characterization, which determines carrier lifetime, ambipolar mobility, carrier drift velocity variation and detector MTF limits, has been developed. This data can be used to model detector performance and to determine the best approach to system design and optimization.

INTRODUCTION

SPRITE detector models are based on inherent material parameters as well as physical detector shape and various system values. SPRITE detector manufacturers typically supply measured data on detector physical shape, detectivity and responsivity. However, they do not supply measured MTF data or the inherent material parameters which determine all of the detector's merit functions. During system (or detector) design and optimization, the detector user must know all of these values to achieve the best overall system performance.

In general, published and manufacturer supplied material values, such as carrier lifetime and ambipolar mobility, are based on bulk material samples prior to detector fabrication. These bulk values vary considerably from lot to lot and can be affected greatly by detector processing. Bulk values are, therefore, unacceptable for modeling purposes and materials data must be taken after detector fabrication. Using post fabrication data, the detector user can adjust the imaging system to deliver optimal performance for a specific detector. In addition, if fabrication processes are well controlled, a detector manufacturer can predict the optimal shape (i.e. bar taper) for future detectors fabricated from the same material lot (with the same bulk parameters), based on the post fabrication material parameters of a sample detector.

A nondestructive method of determining the post fabrication material parameters required for detector and systems modeling, design and optimization has been developed. The test also provides a means of detector MTF measurement which isolates background integration effects and quantifies drift velocity variation at different points along the SPRITE bar. Using the described method, over 200 tests were performed on thermo-electrically cooled, 3-5 μm bifurcated and horn geometry bars of varying lengths, at various temperatures and at two different drift velocities.

0-8194-0597-3/91/$4.00

NOMENCLATURE

D	Diffusion rate (cm^2/s)	t_p	Time delay to pulse peak (μs)
k	Boltzman's constant (J/K)	V_b	Bias voltage (V)
k_s	Spatial frequency (rad/m)	V_p	Peak signal (V)
L	Detector length (μm)	v_d	Drift velocity (m/s)
l_r	Readout length (μm)	v_s	Scan velocity (m/s)
Q_a	Ambipolar diffusion length (cm)	x_c	Spot to readout distance (μm)
q	Electron charge (C)	ϵ	Electric field (V/cm)
T	Temperature (K)	μ	Ambipolar mobility (cm^2/V s)
t_d	Detector dwell time (μs)	τ	Carrier lifetime (μs)

TEST CONCEPT

Both 3-5 and 8-12 μm SPRITE detectors operate on the principle of excess carrier transport in a photoconductive material. Radiation absorbed by the photoconductor generates excess carriers which diffuse and recombine at rates which can be expressed as a point spread function. If a bias is applied, the excess carriers will drift with the carrier flow until recombination or transport out of the photoconductor occurs. During this transit time, several inherent material characteristics affect parameters such as diffusion rate, recombination rate, and drift velocity. These in turn affect the detectivity and minimum resolution of the detector and imaging system.

The material's characteristics in question are interrelated and vary with incident energy, detector temperature and bias voltage. Consequently, a method which determines all of the material characteristics with a single test was desired. An impulse response test was therefore employed. This method has the added advantage of isolating the contribution of scan and drift velocity mismatch to the detector MTF. By performing multiple impulse tests along the length of the detector bar, carrier lifetime and ambipolar mobility can be determined. In general, the test resembles a Haynes-Schockley semiconductor experiment referenced by Sze[1].

To generate an impulse response, a pulsed infrared laser diode was focused at a single point on the detector bar (Figure 1). The use of an extremely short pulse (10 to 100 ns) reduced or eliminated the need for scanning. The output of the diode (4.6 μm peak wavelength) was focused on a 50 μm diameter pinhole which was imaged onto the detector. A cold stop was used to guarantee the same detector FOV as would be experience in the imaging system to be optimized. The imaged spot size was measured and found to be 48 μm in diameter (full width, 1% points). Due to the diode pulse duration (100 ns) and the carrier drift velocity, some horizontal smearing (integration) of the carrier-generated spot occurred. The resultant carrier spot length was calculated to be less than 58 μm for all test cases. Precise spot positioning along the detector bar was achieved with a 6 axis, computer controlled micropositioning system.

Detector temperature and bias voltage were both tightly controlled. A preamp enlarged the detector signal to a usable level and the data was collected, averaged (10 pulses per position) and digitized by an oscilloscope which was triggered by the diode pulse generator (Figure 2). Digitized data was stored on magnetic tape and later transferred to 1.2 Mb disks for analysis. Data reduction was performed using a desktop computer and a combination of custom and commercially available software. The data collection system MTF losses were found to be negligible compared to the detector MTFs and were, therefore, not included in the analysis.

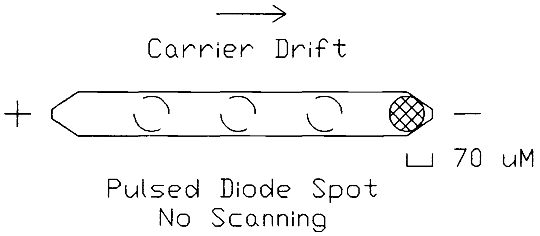

Figure 1
Method of Impulse Generation

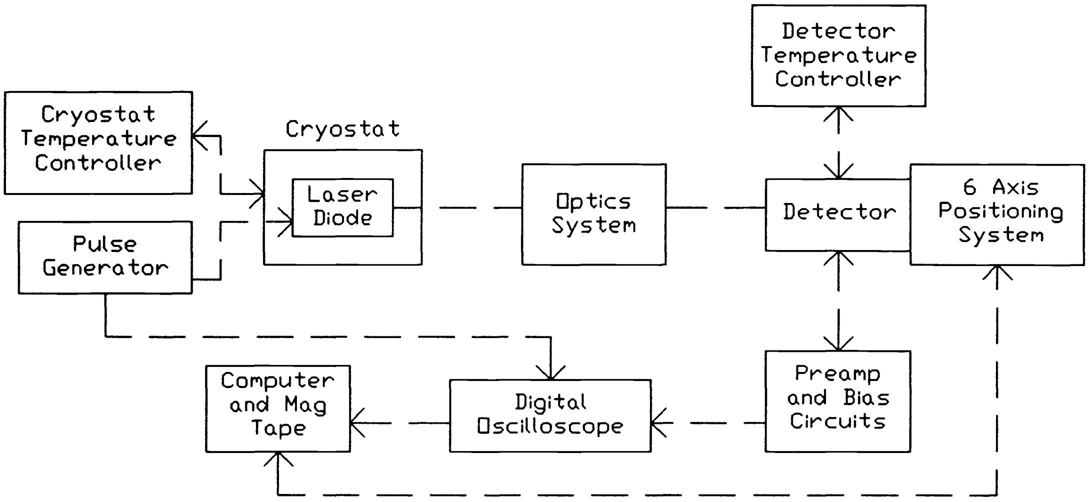

Figure 2
Block Diagram

DATA COLLECTION

After bringing the detector to the desired temperature, the diode spot was imaged near the positive bias contact of a detector bar. The diode was pulsed and the oscilloscope data recorded. The time delay between the diode pulse and the peak preamp output was measured. The average drift velocity was calculated based on the distance between the spot center and the readout center (x_c) as well as the recorded peak time delay (t_p).

$$v_d = \frac{x_c}{t_p} \qquad [1]$$

Through repeated tests, the bias voltage was adjusted to deliver the desired average drift velocity across the bar. The spot was then positioned near the detector readout at the point which delivered the maximum voltage output. Due to the readout shape, this was typically 70 μm from the end of the bar rather than directly on the negative bias contact (Figure 1). The diode was pulsed and data was taken. The spot was then moved toward the positive contact in various increments (typically 100 μm) and the test was repeated. An example of the data gathered on a 650 μm long, horn geometry bar with a 62.5 μm readout is shown in Figure 3. The detector was at 190K and a bias voltage of 2.650 Vdc was applied. The average drift velocity over the full 650 μm length was 66 m/s.

As can be seen in Figure 3, a large negative spike exists at the leading edge of the data. The spike is the result of Radio Frequency Interference (RFI) generated by the laser diode and pulse generator. Data on the spike was recorded with the detector aperture blocked. This yielded the RFI-generated signal alone. The RFI signal was found to be quite consistent for a given detector bar. Further comparison showed that the RFI signal was identical to the negative spike of pulses which were positioned far from the detector readout. The negative spike of these pulses can, therefore, be subtracted from all other pulse data to correct for the RFI error. The results of this subtraction are shown in Figure 4.

DATA REDUCTION

Since the detector length, bias voltage and average drift velocity are known, the average ambipolar mobility and the average electric field can be determined by the following relationship. For the 650 μm bar, under the previously described conditions, the average mobility (over the full 650 μm length) was found to be 161 cm^2/V s and the average electric field was 40.77 V/cm. Quoted values of ambipolar mobility for 3-5 μm material, under these test conditions, typically range from 140 to 150 cm^2/V s.

$$\mu = \frac{v_d}{\epsilon} = \frac{v_d\,L}{V_b} \qquad [2]$$

The carrier lifetime can be calculated from the rolloff of the peak signal as the spot is moved to positions further from the readout. Each spot position produces a pulse at the readout which has been modified by both diffusion and recombination during transit along the bar. At the time the peak signal passes through the readout, the carrier concentration can be written as[2]

$$\delta p(t) = \frac{A}{\sqrt{t_p}} \exp^{-\frac{t_p}{\tau}} , \qquad [3]$$

where A is a constant, τ is the carrier lifetime and t_p is the time at which the peak signal occurs. The measured data and a best fit curve for Equation 3 are shown in figure 5. The fitted curve gives a carrier lifetime of 4.27 μs for the 650 μm detector. Data, provided by the detector manufacturer, also indicated a lifetime of approximately 4.2 μs. This measured carrier lifetime is probably dominated by surface recombination and will not necessarily be the same as the bulk lifetime.

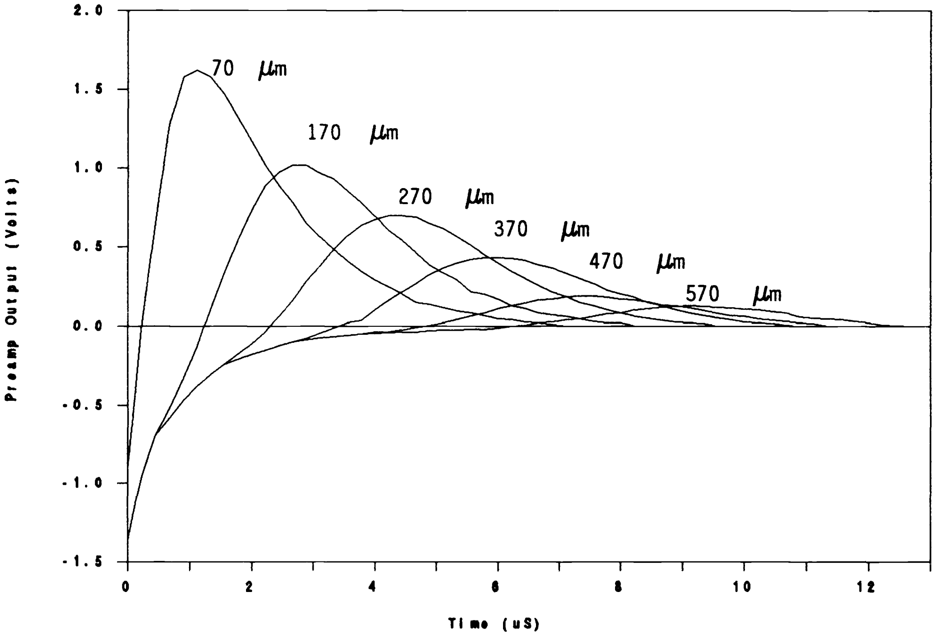

Figure 3
Preamp Output
with RFI Contribution

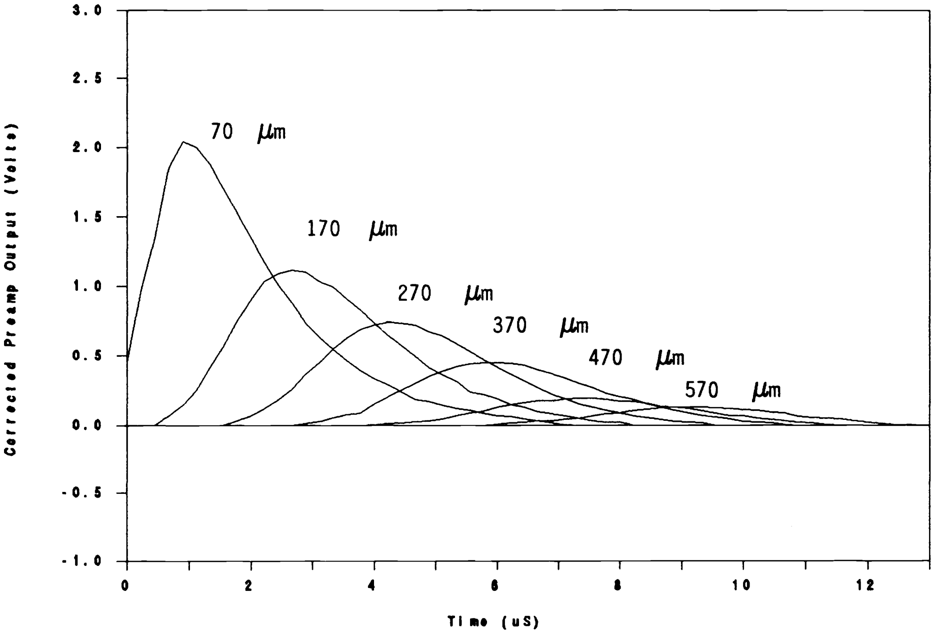

Figure 4
Corrected Preamp Output

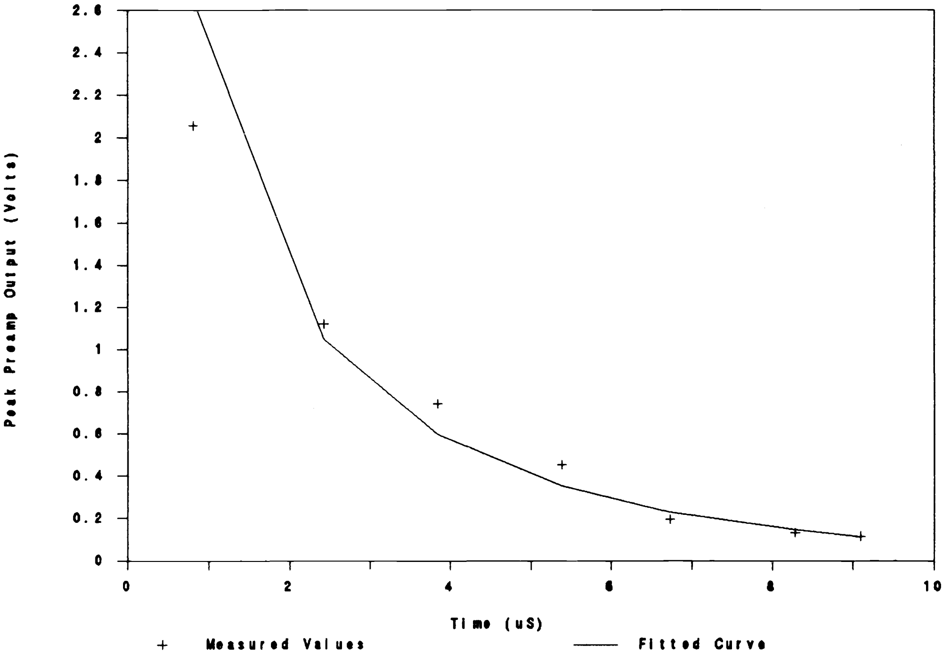

Figure 5
Signal/Carrier Decay

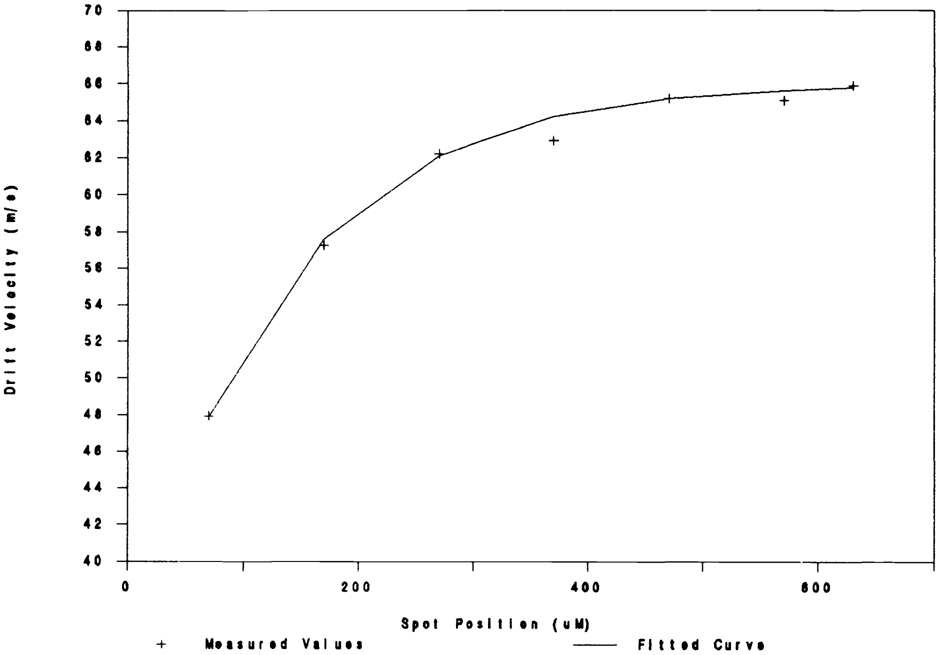

Figure 6
Drift Velocity Variation

Average drift velocity between the spot positions and the readout can be found by applying equation [1]. These values may be plotted to show drift velocity variation along the bar (Figure 6). An equivalent scanning system velocity mismatch can be determined by using a weighted average based on each spot's anticipated contribution to the total signal strength. This equivalent mismatch can then be used in theoretical MTF equations. Weighting values are based on the peak signal strength for each spot position. The equivalent mismatch for the 650 μm bar was found to be 8.3 m/s. In determining this mismatch the following equation was used.

$$V_d = \frac{(V_s-V_{d1})\,V_{p1} + (V_s-V_{d2})\,V_{p2} + \ldots.\,(V_s-V_{dn})\,V_{pn}}{V_{p1} + V_{p2} + \ldots V_{pn}} \qquad [4]$$

Figure 6 indicates a drift velocity variation partially due to background integration. By tapering the bar properly, this variation can be reduced. In this case, maximum velocity variation was greater than 25% across the bar. However, after weighting the variation according to signal strength contribution, the equivalent scanning system mismatch was determined to be 13% (8.3 m/s). Ashley et al. have shown that this variation will increase with longer lifetimes.[3] Previously published data on 8-12 μm detectors, show minor drift velocity variation. Data taken during these tests indicate that 3-5 μm detectors are more susceptible to this phenomenon. Possibly due to the inherently longer carrier lifetime and considerably lower ambipolar mobility in 3-5 μm material.

The spot MTF may be found by the Fourier transform of the impulse response. The MTF for each position can be calculated and plotted (Figure 7). It must be noted that the measured spot MTF is not the detector MTF, but the MTF for one particular spot position. To obtain the overall detector MTF, integration within the bar must be considered. Pulses generated nearer the readout contribute more signal and, therefore, influence the detector MTF more heavily. The signal influence is directly related to the carrier recombination curve and, therefore, the carrier lifetime. Due to the linearity (superposition) characteristics of the Fourier transform, a weighted average, based on the signal contribution of each spot, can again be used to predict overall detector performance. Detector MTF (without velocity mismatch) can be calculated by the following equation.

$$MTF = \frac{MTF_1\;V_{p1} + MTF_2\;V_{p2} + \ldots.MTF_n\;V_{pn}}{V_{p1} + V_{p2} + \ldots.\,V_{pn}} \qquad [5]$$

The optical and electrical MTFs of the imaging system in question were measured separately. These values were combined (multiplied) with the detector MTF which was determined by impulse response testing. The predicted system MTF curve based on these calculations is presented in Figure 8. The measured optical and electrical MTFs were also combined with theoretical detector MTF curves based on material parameters determined by impulse response testing. System performance curves based on these values are also presented in Figure 8. The entire imaging system's performance (end to end including detector) was then measured and the true system MTF is included for reference.

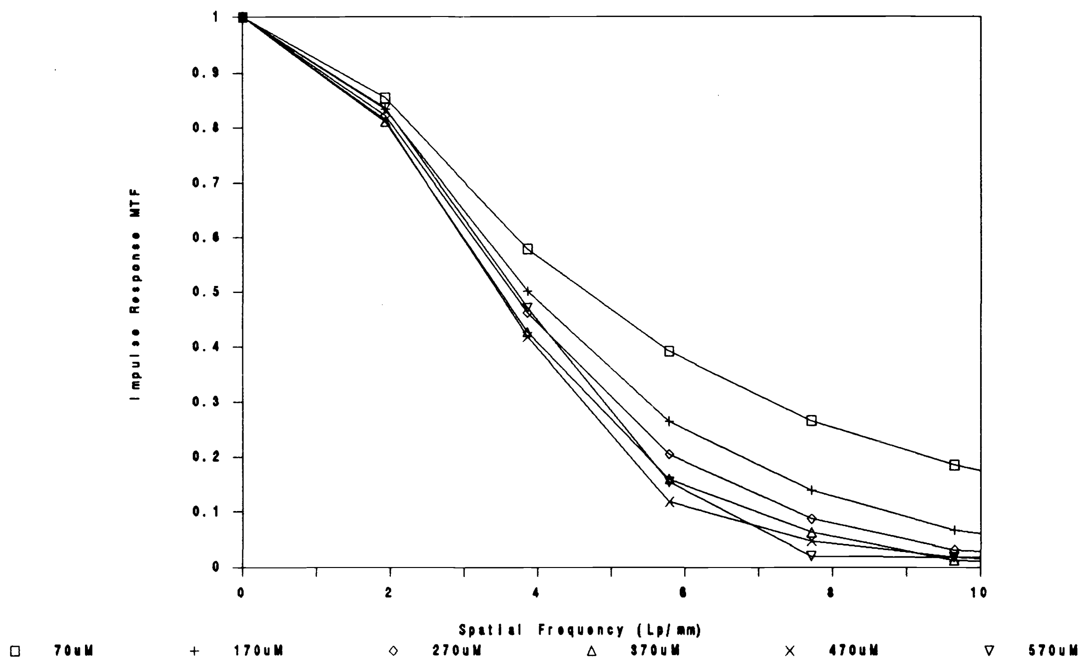

Figure 7
Detector Impulse Response MTF
at Various Spot Positions

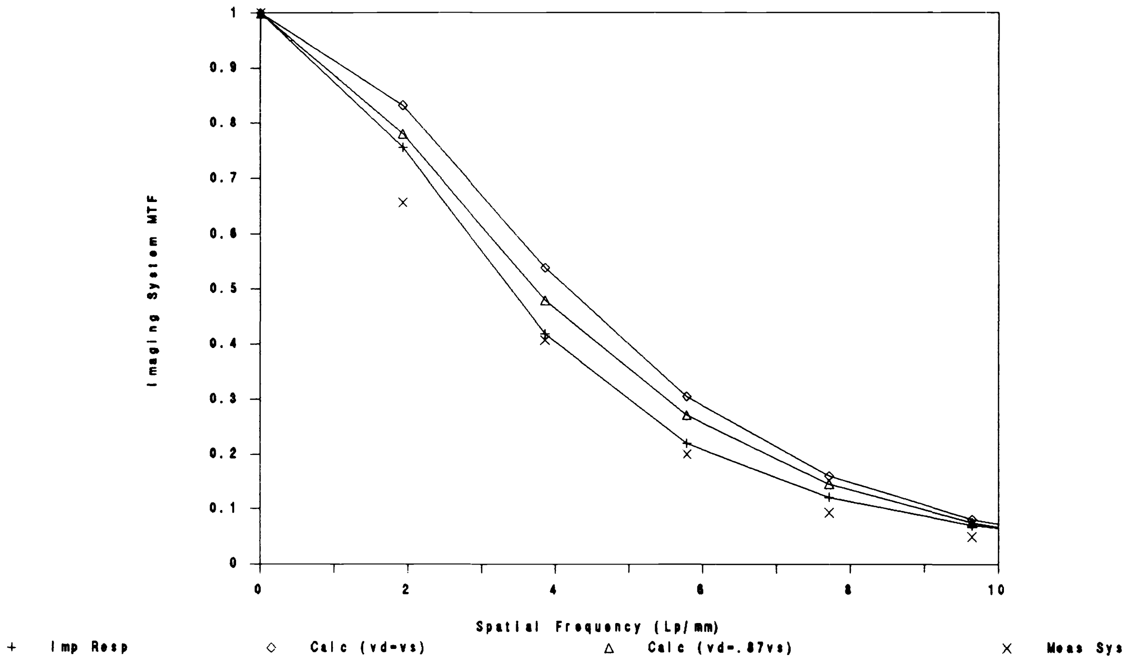

Figure 8
Theoretical and Measured
Imaging System MTF

The equation used for theoretical detector MTF is a combination of two previously published equations. One equation accounts for velocity mismatch[4] but includes no term for finite bar length. The second accounts for a finite detector length[2] but does not address velocity mismatch. Both equations were derived from basic semiconductor physics and are equivalent if velocity mismatch is zero and the detector is of infinite length. Although no lengthy derivation has been attempted, intuitively, the equations can be combined to cover all cases of velocity mismatch and bar length. The combined equation is shown below. Differences between measured and theoretical values are due, in part, to contact accumulation effects which are not addressed in the equation.

$$MTF = \frac{\left[1 - \exp\left(\frac{-L\,(Q_a^2\,k_s^2 + 1)}{\mu\,\epsilon\,\tau}\right)\right]\left[\frac{2\sin\left(\frac{k_s\,l_r}{2}\right)}{k_s\,l_r}\right]}{\left[1 - \exp\left(\frac{-L}{\mu\,\epsilon\,\tau}\right)\right]\left[(Q_a^2\,k_s^2 + 1)^2 + ((v_d - v_s)\,\tau\,k_s)^2\right]^{\frac{1}{2}}} \qquad [6]$$

$$Q_a = (D\,t_d)^{\frac{1}{2}} \qquad for\ \ t_d < \tau$$

$$Q_a = (D\,\tau)^{\frac{1}{2}} \qquad for\ \ t_d \geq \tau$$

$$D = \mu\,\frac{k\,T}{q}$$

SUMMARY

An impulse response test and data evaluation method for SPRITE detectors was introduced and a method of pulse generation was examined. The test and subsequent data reduction delivers measured values of carrier lifetime, average ambipolar mobility, drift velocity variation, and detector MTF. This data can be used to optimize imaging system performance or to tailor future detectors from the same material lot.

Data for one 3-5 μm detector bar, which was 650 μm long with a 62.5 μm horn geometry readout, was presented. The data was taken at 190K with an average drift velocity of 66 m/s. The carrier lifetime was determined to be 4.27 μs, the mobility 161 $cm^2/V\,s$ and the average drift velocity variation 8.3 m/s. Imaging system MTF was predicted using the impulse data and using theoretical calculations. The actual imaging system performance was then compared to the predicted values. Impulse response predictions were considerably more accurate than theoretical predictions. Differences are attributed primarily to contact accumulation effects which are not included in present SPRITE models.

Data collection was supported by McDonnell Douglas Missile Systems Company, Titusville Florida. Special thanks to Mr. W.F. Morgan and his test team for collecting the majority of the impulse response data. This paper has been authorized for public release; unlimited distribution; case # 910989.

REFERENCES

1. S.M. Sze; Physics of Semiconductors; Wiley-Interscience; 1969: 70-71.
2. D. Day and T.J. Shepherd; Transport in Photo-conductors - I; Solid State Electronics 25, 707-712 (1982).
3. T. Ashley, C.T. Elliot, A.M. White, J.T.M. Witherspoon, and M.D. Johns; Optimization of Spatial Resolution in SPRITE Detectors; Infrared Physics 24 (1984): 25-33.
4. G.D. Boreman and A.E. Plogstedt; Modulation Transfer Function and Number of Equivalent Elements for SPRITE Detectors; Applied Optics 27 (15 October, 1988): 4331.